



Structure of jadeite melt at high pressures up to 4.9GPa

Tatsuya Sakamaki, Yanbin Wang, Changyong Park, Tony Yu, and Guoyin Shen

Citation: *J. Appl. Phys.* **111**, 112623 (2012); doi: 10.1063/1.4726246

View online: <http://dx.doi.org/10.1063/1.4726246>

View Table of Contents: <http://jap.aip.org/resource/1/JAPIAU/v111/i11>

Published by the [American Institute of Physics](#).

Related Articles

Investigation of size effects on the structure of liquid GeSe₂ calculated via first-principles molecular dynamics
J. Chem. Phys. **136**, 224504 (2012)

Relating composition, structural order, entropy and transport in multi-component molten salts
J. Chem. Phys. **136**, 144507 (2012)

Note: Anharmonicity of quasi-lattice modes in glass and super-fragile liquid states of decahydroisoquinoline: C₉H₁₇N
J. Chem. Phys. **136**, 136101 (2012)

Studies of structural, dynamical, and interfacial properties of 1-alkyl-3-methylimidazolium iodide ionic liquids by molecular dynamics simulation
J. Chem. Phys. **136**, 124706 (2012)

Calorimetric and relaxation properties of xylitol-water mixtures
J. Chem. Phys. **136**, 104508 (2012)

Additional information on *J. Appl. Phys.*

Journal Homepage: <http://jap.aip.org/>

Journal Information: http://jap.aip.org/about/about_the_journal

Top downloads: http://jap.aip.org/features/most_downloaded

Information for Authors: <http://jap.aip.org/authors>

ADVERTISEMENT

World's Ultimate AFM Experience the Speed & Resolution



The fastest AFM on the planet is now simply the best AFM in the world

[CLICK TO REQUEST INFO](#)

Structure of jadeite melt at high pressures up to 4.9 GPa

Tatsuya Sakamaki,^{1,a)} Yanbin Wang,^{1,b)} Changyong Park,^{2,c)} Tony Yu,^{1,d)} and Guoyin Shen^{2,e)}

¹Center for Advanced Radiation Sources, The University of Chicago, Chicago, Illinois 60637, USA

²HPCAT, Geophysical Laboratory, Carnegie Institution of Washington, Argonne, Illinois 60439, USA

(Received 12 April 2011; accepted 13 November 2011; published online 15 June 2012)

The structure of jadeite ($\text{NaAlSi}_2\text{O}_6$) melts has been studied using multiple-angle energy-dispersive x-ray diffraction up to 4.9 GPa and 1923 K. The first sharp diffraction peak in the structure factor shifts toward higher momentum transfer as pressure increases, indicating the shrinkage of the intermediate network in the melt. The radial distribution function shows a monotonous decrease in average T-T length and T-O-T angle with increasing pressure, but displays no detectable change in the average bond length between tetrahedrally coordinated cations and oxygen (T-O length, where $\text{T} = \text{Si}^{4+}$, Al^{3+}). Our observations indicate that the dominant structural changes occur in the intermediate range order at pressures up to 4.9 GPa. The changes in T-O length, T-T length, and T-O-T angle appear to correlate with the viscosity anomaly in this pressure range. © 2012 American Institute of Physics. [<http://dx.doi.org/10.1063/1.4726246>]

INTRODUCTION

Structural properties of silicate melts have close relationship with physical, chemical, and thermal properties of magmatic liquids.^{1–3} Our understanding of the formation and evolution of magma in the Earth and terrestrial planets, igneous processes, as well as volcanism depends critically on the knowledge of these properties.^{4,5}

A marked decrease in viscosity with increasing pressure was observed in aluminosilicate melts by Kushiro,^{5–7} who suggested that a change in aluminum coordination in the melt from fourfold to sixfold, with an accompanying decrease in the degree of polymerization of the melt, is responsible for this anomalous behavior. Since the report (Ref. 5), glass structure of jadeite has been investigated at high pressures to understand the mechanism of the viscosity change. Based on the observation of infrared vibrational spectra and a shift in both Al K_{α} and K_{β} radiation, a change in coordination number of aluminum from four to six was reported.⁸ However, a study using Raman spectra did not support this conclusion.⁹ The latter compared Raman spectrum of jadeite glass at 1 atm with that of quenched glass from 4.0 GPa and concluded that Al remains tetrahedrally coordinated throughout this pressure range. The structure of jadeite glass quenched from 1.0 GPa was also studied using radial distribution analysis and no evidence of increased coordination number in aluminum was found at this pressure.¹⁰ However, aluminum K-edge x-ray absorption near edge structure (XANES) spectra of jadeite glass by Ref. 11 provided evidence for a pressure-induced coordination change of Al, showing that jadeite glass synthesized at 4.4 GPa contained about 6% of each ^vAl and ^{vi}Al. In all of these studies, the samples were quenched glasses recovered from high temperature and high

pressure. Direct *in situ* structure measurements of jadeite melt at high pressure-temperature conditions are still lacking.

The high melting points and weak scattering power impose significant difficulties in studying silicate melt structures with x-rays: A combination of stable and homogeneous heating over a large sample volume and a widely open access to the x-ray scattering angle has been a challenge for the *in situ* measurements. Recent progresses in utilizing the large volume press have made it possible to measure structure changes in magmas up to about 6 GPa and 2390 K.^{12–14} In this study, we report structure data of jadeite melt at high pressures and high temperatures using an energy-dispersive x-ray diffraction (EDXD) method and show the structure evolution with pressure up to 4.9 GPa and 1923 K.

EXPERIMENTAL

Reagent-grade oxides (SiO_2 , Al_2O_3) and crystalline powder of $\text{Na}_2\text{Si}_2\text{O}_5$, which was previously synthesized from Na_2CO_3 and SiO_2 , were mixed in jadeite composition ($\text{NaAlSi}_2\text{O}_6$) in an agate mortar with acetone for 2 h. The mixed powder was melted at 1673 K for 5 min. Crushing and fusing were repeated three times in order to homogenize the starting material.

High pressure and high temperature x-ray diffraction measurements were carried out using the EDXD method at the HPCAT 16-BM-B beamline, Advanced Photon Source. Compressing and melting a large volume of jadeite sample were achieved by using a Paris-Edinburgh press (model VX3) installed in the center of a large Huber rotation stage for *in situ* x-ray measurement. A schematic illustration of the high-pressure and high-temperature cell assembly is shown in Figure 1. The outer pressure media consisted of machinable zirconia (ZrO_2) pallets and sintered boron-epoxy. Machinable magnesia (MgO) in cylinder shape was placed between the boron-epoxy gasket and the graphite heater for protection, heat insulation, and x-ray transparency. Graphite capsule was used as the sample container, insulated by a

^{a)}sakamaki@cars.uchicago.edu. Tel.: 630-252-0430. Fax: 630-252-0443.

^{b)}wang@cars.uchicago.edu. Tel.: 630-252-0425. Fax: 630-252-0443.

^{c)}cpark@ciw.edu. Tel.: 630-252-0477. Fax: 630-252-0496.

^{d)}tyu@cars.uchicago.edu. Tel.: 630-252-6148. Fax: 630-252-0443.

^{e)}gshen@ciw.edu. Tel.: 630-252-0429. Fax: 630-252-0496.

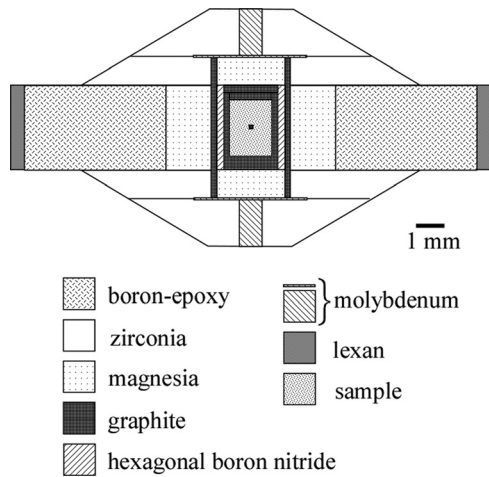


FIG. 1. A cross section of the cell assembly. Black square in the sample is the position of the incident beam.

hexagonal boron nitride (hBN) sleeve and MgO plugs placed on top and bottom of the capsule. Pressures were determined by the equation of state of MgO, proposed by Ref. 15. Temperature was estimated using the relationship calibrated by electric power in a separate temperature calibration experiment with the same cell assembly.

16-BM-B is a bending magnet beamline which provides white x-rays (5–120 keV) with high brightness. The incident x-ray was collimated by two sets of vertical (0.1 mm) and horizontal (0.1 mm) slits. The diffracted signal was collimated with a 0.1 mm gap collimator 80 mm downstream from the sample and a 0.1 mm \times 5.0 mm receiving slit 400 mm further downstream from the scattering slit. The scattered x-rays were detected using a Ge solid state detector (Ge-SSD) with a 4096 multi-channel analyzer. The Ge-SSD was mounted on a two-theta arm on the large Huber rotation stage with air pads, which allowed accurate control on the two-theta angle. Diffraction patterns were collected at 12 fixed diffraction angles ($2\theta = 3^\circ, 4^\circ, 5^\circ, 7^\circ, 9^\circ, 11^\circ, 15^\circ, 20^\circ, 25^\circ, 30^\circ, 35^\circ, 39.5^\circ$). Figure 2 shows the schematic diagram of the experimental setup. Collecting time varied with the diffraction angles, as intensities decreased with increasing angle. All patterns were collected until the maximum intensity reached at least 2000 counts. An example of diffraction patterns of jadeite melt is shown in Figure 3.

The structure factors, $S(Q)$ s, were obtained from the measured x-ray diffraction data using an analytical program by Ref. 16 according to the formula,

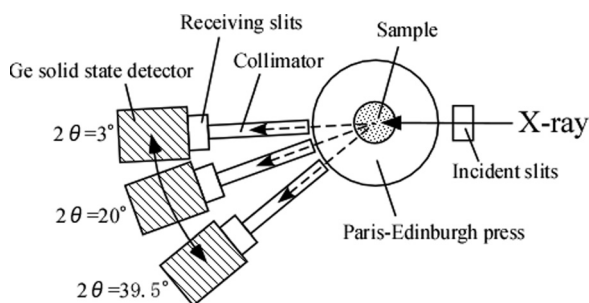


FIG. 2. Schematic diagram of the experimental setup at the 16-BM-B beamline of the APS.

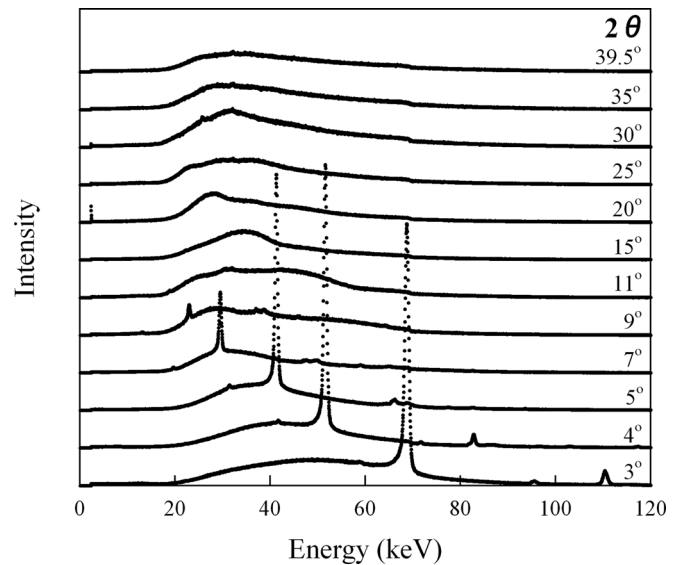


FIG. 3. An example of data set collected at 0.1 GPa and 1473 K. Sharp peaks represent diffraction of graphite used for the sample container and boron nitride which surrounds the container.

$$S(Q) = \left\{ I^{coh}(Q) - \sum_{j=1}^m f_j^2(Q) \right\} / \left\{ \sum_{j=1}^m f_j(Q) \right\}^2, \quad (1)$$

where $I^{coh}(Q)$ is the coherent intensity resulting from the correlations of atoms, $f_j(Q)$ is the atomic scattering factors of the j -th atom, and the summation is taken over the formula unit. Q is scattering vector, expressed as,

$$Q = 4\pi \sin\theta / \lambda = 4\pi E \sin\theta / hc, \quad (2)$$

where λ , E , θ , h , and c are the wavelength, energy of the x-rays, diffraction angle, Planck's constant, and the speed of light in vacuum, respectively. The local structures in real space are given by the radial distribution function, $G(r)$, as proposed by Ref. 17, obtained by taking the Fourier transform of $S(Q)$:

$$G(r) = \frac{2}{\pi} \int_0^{Q_{max}} Q \{S(Q) - 1\} \sin(Qr) dQ, \quad (3)$$

where r is the radial distance. More details of the analysis method are described in elsewhere.¹⁴

RESULTS AND DISCUSSION

Structure measurements of jadeite melt were carried out in the pressure range from 0.1 to 4.9 GPa at 1473 to 1923 K. We have collected XRD data of the melt with Q up to 14 \AA^{-1} . In general, measuring the energy dispersive diffraction data at higher 2θ angle (e.g., Fig. 3) enhances the quality of data in terms of the real-space resolution, proximity to the full scattering condition, and the minimal oscillatory features benefitting the estimation of the incident white x-ray spectrum. In our data analysis, the estimation of the incident spectrum based on the Monte Carlo algorithm¹⁶ was benefited by the high angle data; however, the maximum Q of the

structure factor reduced from all measured data including the highest 2θ angle was practically limited due to unresolved systematic errors. The extracted structure factor, $S(Q)$, of which the Q_{max} was chosen to obtain a self-consistent reliability criteria as described in Ref. 18, are shown in Figures 4(a) and 4(b). The first peak (typically centered around $1\text{--}3 \text{ \AA}^{-1}$), generally referred to as “first sharp diffraction peak (FSDP),” is in general a signature of the intermediate-range order in the silicate network.¹⁹ The positive pressure dependence of FSDP in Q -space represents a decrease in the intermediate correlation distances in real space with pressure. Figures 4(b) and 4(c) show that FSDP of jadeite melts moves towards higher- Q monotonically with increasing pressure up to 4.9 GPa, suggesting continuous shrinkage of the network structure, especially in terms of the intermediate range ordering. The FSDP position changes from $1.93(1) \text{ \AA}^{-1}$ at 0.1 GPa to $2.09(1) \text{ \AA}^{-1}$ at 4.9 GPa. This suggests that the average intermediate-range correlation corresponding to around 3.1 \AA at 4.9 GPa has been reduced by 8% compared to the melt at 0.1 GPa. This structural change may play an important role in the decrease of viscosity of the melt.²⁰ Figure 4(c) also shows the FSDPs for MgSiO_3 and CaSiO_3 melts for comparison.^{12,21} Both lengths and pressure dependence of the FSDP for jadeite melt appear to be rather similar to that of Al-free MgSiO_3 melt. The FSDP of CaSiO_3 melt, on the other hand, shows strong non-linear pressure dependence. Several studies reported the appearance of a second sharp diffraction peak (SSDP) between the FSDP and the main peak located around 5 \AA^{-1} .^{12,13,22–24} In this study, our data show no evidence for the presence of the SSDP (Fig. 4(b)).

The local structure of a melt can be obtained from the reduced pair distribution function, $G(r)$, calculated by Fourier transformation of $S(Q)$ (Eq. (3)). Figure 5(a) shows variations of $G(r)$ of jadeite melt with pressure. The $G(r)$ functions are presented after the window function known as Lorch function, $M(Q) = \sin(\Delta r Q)/(\Delta r Q)$ where $\Delta r = \pi/Q_{max}$, is convoluted to get rid of the truncation errors. The peak at around $1.6\text{--}1.7 \text{ \AA}$ corresponds to the bond length between tetrahedrally coordinated cation ($T = \text{Si}^{4+}$, Al^{3+}) and oxygen (T-O length) in the jadeite melt. The peak at around 2.9 \AA represents the bond length between two tetrahedrally coordinated cations (T-T length). The real-space resolution for the bond length correlation, based on the $\Delta r = \pi/Q_{max}$ consistent with the window function, is around 0.2 \AA in our measurement. The differences between individual Si-O and Al-O bond lengths are not readily resolved if smaller than this scale. The observed bond length around $1.6\text{--}1.7 \text{ \AA}$ does not show any distinctive features that can separate out Si-O and Al-O correlation with this 0.2 \AA resolution, therefore, represents the average of Si-O and Al-O distances. The T-O bond length information, however, is important for understanding the nature of the TO_4 tetrahedron, which is the basic unit of the silicate melt. Figure 5(b) shows the T-O length as a function of pressure for jadeite melt and the comparison with MgSiO_3 and CaSiO_3 melts. For jadeite melt, T-O length decreases between 0.1 and 2.5 GPa and then levels off. The change in T-O length gives an indication of the change of tetrahedrally coordinated cations. It is known that octahedrally coordinated T cations have longer bond lengths than

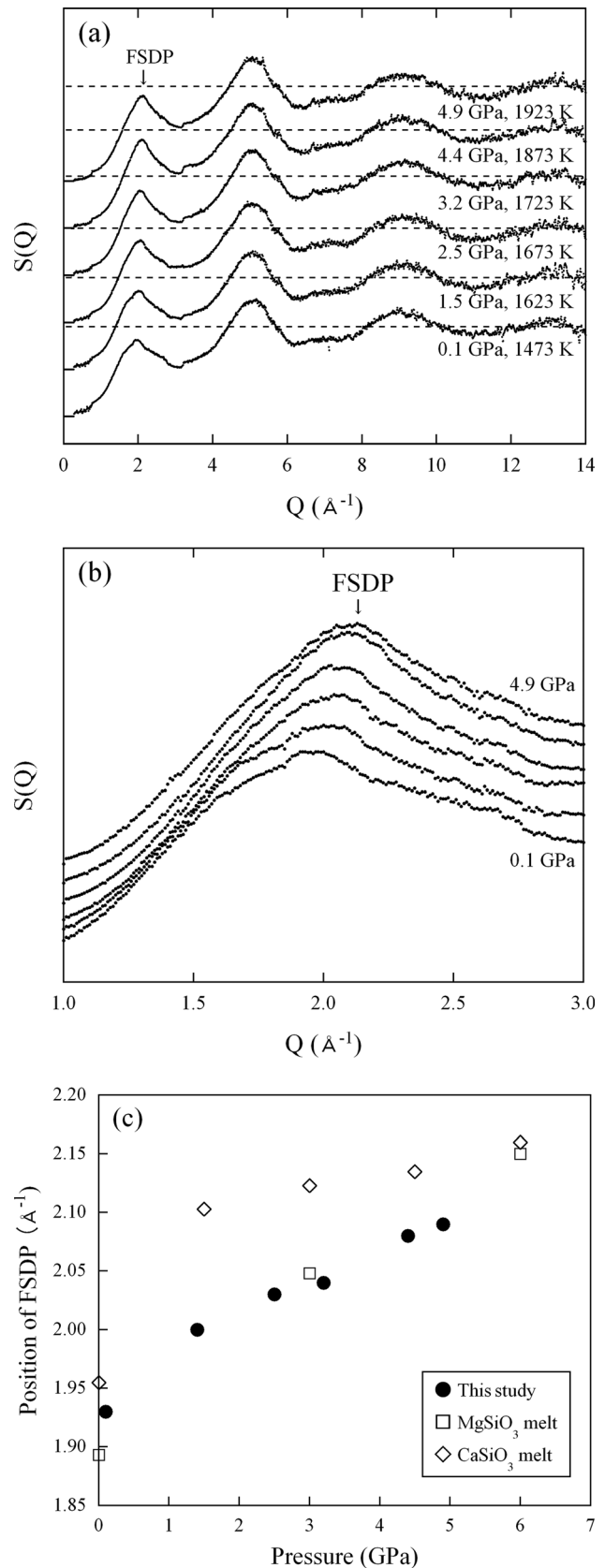


FIG. 4. (a) Structure factors $S(Q)$ of jadeite melt with pressure. The arrow indicates the FSDP. (b) Magnified view of $S(Q)$ with pressure in the range between 1 and 3 \AA^{-1} . (c) Pressure dependence of FSDP in $S(Q)$. The solid circles are results of this study. The data of MgSiO_3 melt (open squares) and CaSiO_3 melt (open diamonds) at high pressure are from Ref. 12, and data at 1 atm are from Ref. 20.

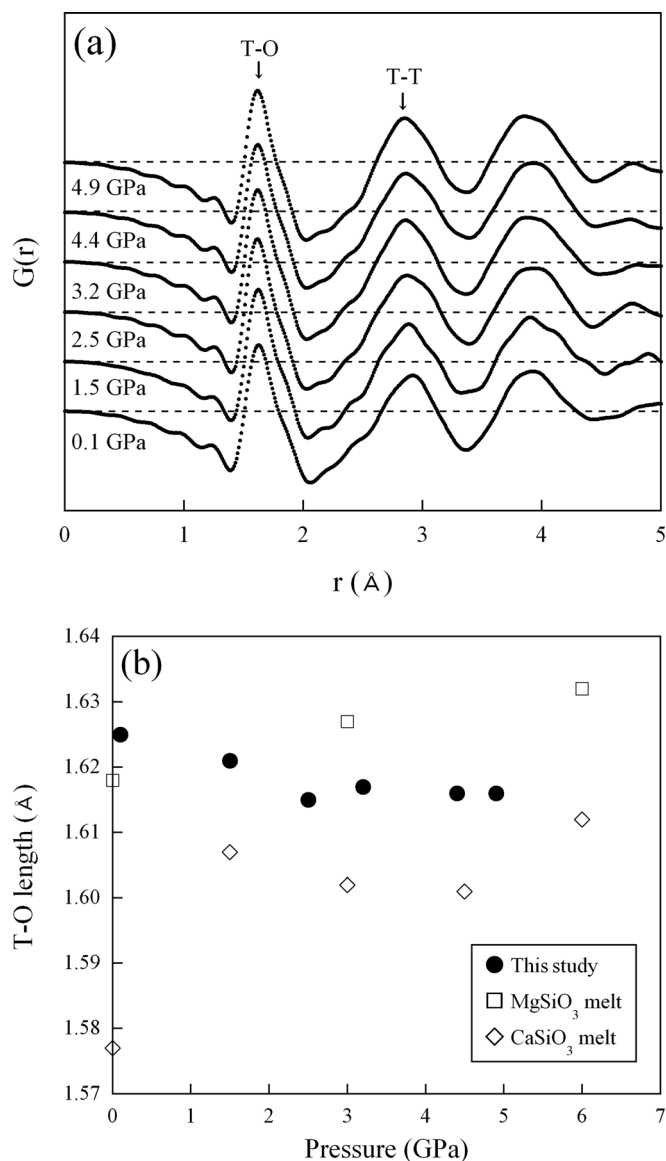


FIG. 5. (a) Radial distribution function $G(r)$ of jadeite melt with pressure. The peak positions indicate the average bond length of the atomic pairs in the melt. The arrows show the peak positions of T-O, O-O, and T-T. (b) Pressure dependence of T-O length in jadeite melt (solid circles) and comparison with Si-O length in the MgSiO₃ melt (open squares) and CaSiO₃ melt (open diamonds). The data of MgSiO₃ and CaSiO₃ melt at high pressure are from Ref. 12, and data at 1 atm are from Ref. 20.

tetrahedrally coordinated ones.²² If the coordination number of Al increases, the T-O peak should exhibit some separation between ^{IV}Si-O and ^{V,VI}Al-O peaks. However, we cannot resolve such a separation in the peak of T-O length. In fact, not even slight shape change in the T-O peak was detected within the 0.2 Å experimental resolution. This indicates that the change of aluminum coordination number does not occur under the current experimental condition. There is a possibility, however, that the Q range is not sufficient for the required resolution in $G(r)$. Therefore, we conclude that the proportion of the highly coordinated Al is too small to be detected within our experimental resolution.

T-T bond length reflects the relationship of one TO₄ tetrahedron unit with respect to the neighboring ones and therefore is significant in the discussion of the 3 dimensional (3D)

nature of the melt structure. Average T-O-T angle was calculated using the relationship between T-O bond length and T-T bond length ($\text{T-O-T angle} = 2\arcsin\{[T-T]/2[T-O]\}$), assuming corner-sharing TO₄ tetrahedra forming a 3D framework structure (Figure 6). Figure 7(a) illustrates the pressure dependence of T-O length, T-T length, and T-O-T angle in the jadeite melt. T-T length decreases with pressure much faster than does T-O bond length. The T-O-T angle exhibits a similar trend to that for T-T: it changes from 129.1° at 0.1 GPa to 123.0° at 4.9 GPa, a 5.0% decrease. As T-O-T angle is closely related to the intermediate-range network structure, the decrease in T-O-T angle indicates a change to a more compact structure. This result is rather similar to the behavior of crystalline SiO₂ polymorphs with ^{IV}Si. Quartz consists of mainly six-member rings and its Si-O-Si angle is 143.7°,²⁵ whereas in the case of coesite, which is a high-pressure phase, SiO₄ tetrahedra form four-member rings and Si-O-Si angle is 137.4° (a 4.6% decrease).²⁶

The ratio between the number of non-bridging oxygen anions (NBO) and that of tetrahedrally coordinated cations (T), commonly referred as NBO/T, is an important indicator for structures of silicate glasses and melts (NBO/T=4: a monomer, 3: a dimer, 2: a chain, 1: a sheet). If NBO/T equals zero, such is the case for jadeite melt, all tetrahedra are interconnected via four oxygen anions and a three-dimensional network structure is formed.²⁷

Structure of crystalline jadeite is monoclinic with parallel sheets of octahedrally coordinated aluminum and 8-coordinated sodium polyhedra connected by silicate chains. Si-O-Si angle of jadeite crystal is 139.3°,²⁸ which is larger than the T-O-T angle of jadeite melt at 0.1 GPa. The structure of jadeite melt differs significantly from that of the crystalline counterpart in terms of Al coordination. Al has 6-fold coordination in crystalline jadeite, but is intermediate in jadeite glass and melt. Thus, Al can act as both network former and modifier, depending on the silicate composition.²⁹ In silicate melts that contain alkali metal cations and/or alkaline-earth metal cations, Al cations act as network formers like Si. The ratio of Al/Na in the jadeite equals to 1, which suggests that all Al cations act as network formers, with pairing, interstitial Na to maintain the charge balance.

The decrease in T-O-T angle and intermediate range ordering distances suggests that the topology of tetrahedral connectivity changes toward a more compact network structure. The topological changes include the breaking and re-bonding of T-O-T connection to make smaller member rings. This structural change in turn influences properties of the

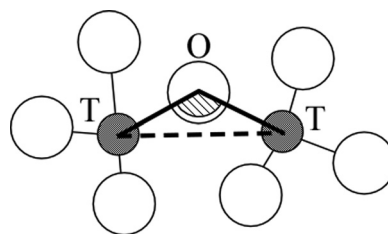


FIG. 6. Schematic diagram of the connection for TO₄ tetrahedra. Grey and white spheres show tetrahedrally coordinated cations (T) and oxygen (O), respectively. Heavy line is T-O bond length, and heavy broken line is T-T bond length. A sector with diagonal lines indicates the T-O-T angle.

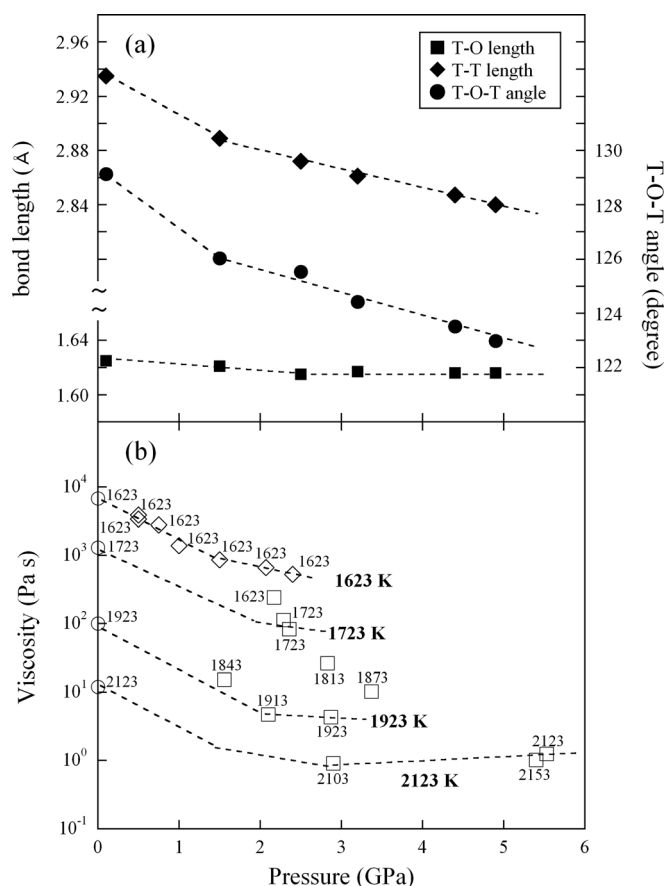


FIG. 7. (a) Pressure dependence of T-O length (solid squares), T-T length (solid diamonds), and T-O-T angle (solid circles) in jadeite melt. (b) Pressure dependence of the viscosity of jadeite melt. The numbers indicate temperature in kelvin. The open squares and open diamonds are viscosities at high pressure by Refs. 5 and 27, respectively. The open circles are viscosities at 1 atm calculated using the equation by Ref. 25.

melt, for example viscosity, because the connectivity of T-O-T networks is a controlling factor of the viscosity of a melt.³⁰ Recently, the viscosity measurement of jadeite melt up to 5.5 GPa is reported.³¹ These results showed that the viscosity decreases rapidly to 2.2 GPa, after which the changes are minimal up to 5.5 GPa (Fig. 7(b)). In our diffraction data, we find that the shrinkage of intermediate-range network correlates with the viscosity change up to 4.9 GPa (Fig. 7). This correlation may be explained by two competing factors. First, the breakage of T-O-T bonds in the network may result in a negative dependence of viscosity on pressure.³⁰ Second, closer packing of atoms in general exerts a positive effect in pressure dependence of viscosity.³² For jadeite melt, the breakage of T-O-T bonds may be dominant at low pressures (below ~2 GPa), and thus may have caused a strong negative pressure effect on viscosity. As packing efficiency increases with pressure, the positive pressure effect due to void space reduction may play a more important role above 2 GPa, leading to a weak pressure dependence of viscosity above 2 GPa and even a positive pressure dependence above 4 GPa (Fig. 5(b)). More systematic study is desired to examine the two competing effects for a better understanding of the structure-viscosity correlation.

ACKNOWLEDGMENTS

The authors thank two anonymous reviewers for their constructive comments on the original manuscript. The experiments were performed at HPCAT Sector 16 at the Advanced Photon Source (APS), Argonne National Laboratory. HPCAT is supported by CIW, CDAC, UNLV, and LLNL through funding from DOE-NNSA, DOE-BES, and NSF. APS is supported by DOE-BES, under Contract No. DE-AC02-06CH11357. The PEP system was developed at GeoSoilEnviroCARS (Sector 13), APS. GeoSoilEnviroCARS is supported by the National Science Foundation Earth Sciences (EAR-0622171) and Department of Energy-Geosciences (DE-FG02-94ER14466). Y.W. and G.S. acknowledge the support from COMPRES and NSF Grant Nos. EAR 0711057 and EAR 0738852 for the development of this facility. We thank Curtis Kenny-Benson (HPCAT) for his support during the experiments and Akio Suzuki (Tohoku Univ.) for the starting material.

- ¹B. O. Mysen, D. Virgo, and F. A. Seifert, *Rev. Geophys. Space Phys.* **20**, 353, doi:10.1029/RG020i003p00353 (1982).
- ²B. O. Mysen, D. Virgo, and F. A. Seifert, *Am. Mineral.* **70**, 88 (1985).
- ³I. Kushiro and B. O. Mysen, *Geochim. Cosmochim. Acta* **66**, 2267 (2002).
- ⁴E. Ohtani, *Phys. Earth Planet. Inter.* **38**, 70 (1985).
- ⁵I. Kushiro, *J. Geophys. Res.* **81**, 6347, doi:10.1029/JB081i035p06347 (1976).
- ⁶I. Kushiro, *Earth Planet. Sci. Lett.* **41**, 87 (1978).
- ⁷I. Kushiro, H. S. Yoder, Jr., and B. O. Mysen, *J. Geophys. Res.* **81**, 6351, doi:10.1029/JB081i035p06351 (1976).
- ⁸B. Velde and I. Kushiro, *Earth Planet. Sci. Lett.* **40**, 137 (1978).
- ⁹S. K. Sharma, D. Virgo, and B. O. Mysen, *Am. Mineral.* **64**, 779 (1979).
- ¹⁰M. F. Hochella, Jr., and G. E. Brown, Jr., *Geochim. Cosmochim. Acta* **49**, 1137 (1985).
- ¹¹D. Li, R. A. Secco, G. M. Bancroft, and M. E. Fleet, *Geophys. Res. Lett.* **22**, 3111, doi:10.1029/95GL03175 (1995).
- ¹²N. Funamori, S. Yamamoto, T. Yagi, and T. Kikegawa, *J. Geophys. Res.* **109**, B03203, doi:10.1029/2003JB002650 (2004).
- ¹³A. Yamada, T. Inoue, S. Urakawa, K. Funakoshi, N. Funakoshi, T. Kikegawa, H. Ohfuji, and T. Irifune, *Geophys. Res. Lett.* **34**, L10303, doi:10.1029/2006GL028823 (2007).
- ¹⁴A. Yamada, Y. Wang, T. Inoue, W. Yang, C. Park, T. Yu, and G. Shen, *Sci. Instrum.* **82**, 015103 (2011).
- ¹⁵S. Speziale, C. Zha, T. S. Duffy, R. J. Hemley, and H. K. Mao, *J. Geophys. Res.* **106**, 515, doi:10.1029/2000JB900318 (2001).
- ¹⁶K. Funakoshi, Ph.D. dissertation (Tokyo Institute of Technology, 1997).
- ¹⁷R. Kaplow, S. L. Strong, and B. L. Averbach, *Phys. Rev. A* **138**, 1336 (1965).
- ¹⁸Y. Waseda, *The Structure of Non-Crystalline Materials* (McGraw-Hill, 1980), Chap. 2, p. 327.
- ¹⁹Y. S. R. Elliott, *Nature* **354**, 445 (1991).
- ²⁰I. Kushiro, *J. Geophys. Res.* **91**, 9343, doi:10.1029/JB091iB09p09343 (1986).
- ²¹Y. Waseda and J. M. Toguri, in *Dynamic Process of Material Transport and Transformation in the Earth's Interior*, edited by F. Matumoto (Terra Scientific, Tokyo 1990), p. 37.
- ²²S. R. Elliott, *Phys. Rev. B* **51**, 8599 (1995).
- ²³C. Meade, R. J. Hemley, H. K. Mao, *Phys. Rev. Lett.* **69**, 1387 (1992).
- ²⁴A. Yamada, T. Irifune, H. Sumiya, Y. Higo, T. Inoue, and K. Funakoshi, *High Press. Res.* **28**, 255 (2008).
- ²⁵L. Levien, C. T. Prewitt, and D. J. Werdner, *Am. Mineral.* **65**, 920 (1980).
- ²⁶L. Levien and C. T. Prewitt, *Am. Mineral.* **66**, 324 (1981).
- ²⁷F. Seifert, B. O. Mysen, and D. Virgo, *Am. Mineral.* **67**, 697 (1982).
- ²⁸C. T. Prewitt and C. W. Burnham, *Am. Mineral.* **51**, 956 (1966).
- ²⁹E. F. Riebling, *J. Chem. Phys.* **44**, 2857 (1966).
- ³⁰B. O. Mysen, D. Virgo, C. M. Scarfe, and D. J. Cronin, *Am. Mineral.* **70**, 487 (1985).
- ³¹A. Suzuki, E. Ohtani, H. Terasaki, K. Nishida, H. Hayashi, T. Sakamaki, Y. Shibazaki, and T. Kikegawa, *Phys. Chem. Miner.* **38**, 59 (2011).
- ³²H. Taniguchi, *Mineral. Petrol.* **49**, 13 (1993).